

X-ray emission characteristics of plasmas created by a high-intensity CO₂ laser

G. D. Enright, N. H. Burnett, and M. C. Richardson

National Research Council of Canada, Division of Physics, Ottawa, K1A 0R6, Canada
(Received 11 May 1977; accepted for publication 1 August 1977)

The spectrum of the x-ray continuum and line emission emanating from Al, Mg, and (CH₂)_n plasmas created with a nanosecond CO₂ laser pulse has been investigated at irradiance levels up to 2×10^{14} W/cm².

PACS numbers: 52.50.Jm, 52.25.Ps, 52.70.Kz

Characterization of the x-ray emission from plasmas produced by high-irradiance lasers has proven to be a powerful diagnostic of radiation absorption processes, energy transport, and superthermal electron generation. A precise understanding of these phenomena is demanded in current laser fusion investigations, and already many measurements of the spatial and spectral x-ray emission from plasmas created by short-pulse high-power Nd:glass lasers have been reported.¹⁻⁴ However, up to the present time, little published data exists on the character of the x-ray emission from plasmas produced by CO₂ lasers of comparable irradiance levels.

In this letter we describe initial measurements of the spectral properties of the x-ray continuum and line emission emanating from Al, Mg, and (CH₂)_n plasmas, created with one beam of the COCO-II laser facility,⁵ at irradiance levels up to 2×10^{14} W/cm². In particular, we report measurements of the dependence of x-ray conversion efficiency on laser power, the effect of laser prepulse radiation on continuum and line emission, and measurements of the characteristic temperatures of the thermal and nonthermal plasma components.

The laser system provided energy up to 60 J in a 1.5–2-ns (FWHM) pulse in a near-diffraction-limited beam 80 mm in diameter. This was focused onto plane flat massive targets by means of a 20-cm focal length

off-axis parabolic mirror. The measured focal spot size of ~ 170 μ m in diameter was limited by imperfections in the focusing mirror. The target surfaces were optically polished and tilted $\sim 20^\circ$ from the normal to the incident beam. Prepulse radiation and prelude radiation were carefully monitored each shot with a technique⁵ which permitted the detection of prepulse energies greater than 100 μ J and prelude powers greater than 100 kW. Interferometric studies have confirmed that at these prepulse and prelude levels no detectable plasma density exists (that is $n_e < 10^{18}$ /cm³) prior to the arrival of the main laser pulse.⁶

The extent of the x-ray emitting region of the plasma was deduced from pinhole photographs. The emitting region is ~ 200 μ m in diameter and extends from the surface by no more than 100 μ m. From spatially resolved electron density measurements⁶ it is deduced that the primary x-ray emitting region is restricted to a zone well behind the critical density.

The dependence of the total x-ray emission and the absolute x-ray conversion efficiency on laser irradiance was determined with the use of surface barrier detectors and calibrated thermoluminescent detectors⁷ (TLD's). Figure 1 shows the dependence of the x-ray intensity transmitted through 50- μ m Be foil and 50- μ m Al foil on the incident energy E . In both cases the intensity is proportional to $E^{4/3}$. Since the Al foil does not transmit the intense line emission emitted by the Al plasma, it can be estimated that between 30 and 40%

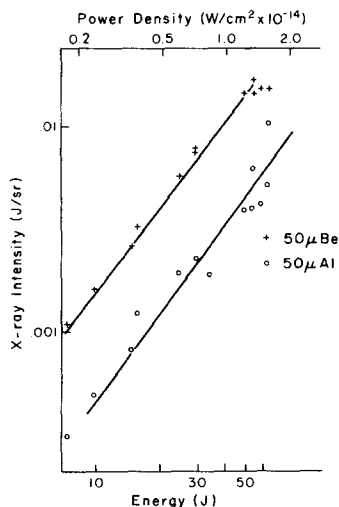


FIG. 1. The dependence of the x-ray emission on incident energy.

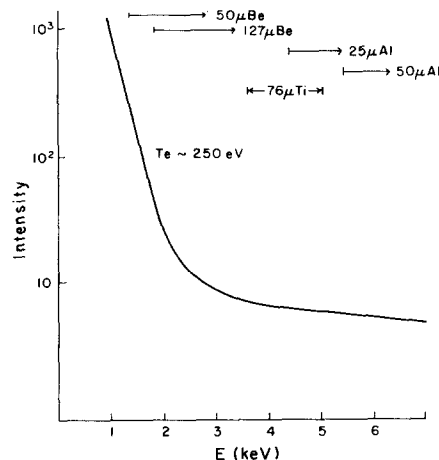


FIG. 2. Continuum spectrum obtained from a (CH₂)_n plasma. Shown are the ranges of the x-ray channels that were used.

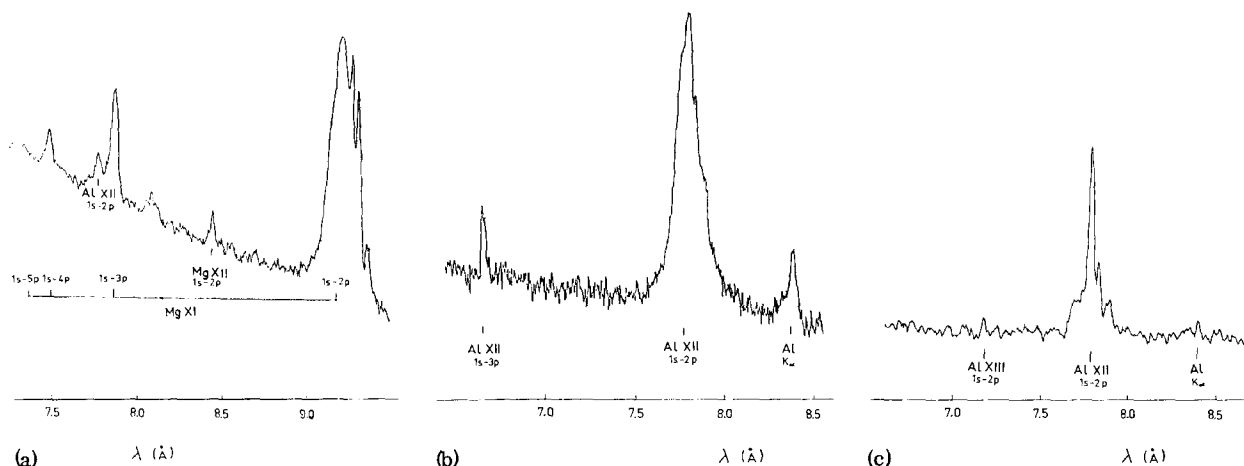


FIG. 3. Microdensitometer scan of (a) a Mg spectrum (8-shot exposure), (b) an Al spectrum (5-shot exposure), and (c) an Al spectrum (single-shot exposure). The laser energy per shot was ~ 40 J in (a) and (b) and 50 J in (c).

of the total x-ray emission that is transmitted through $50\text{-}\mu\text{m}$ Be foil is in the form of line emission. The conversion efficiency of laser energy to x-ray energy transmitted through $25\text{-}\mu\text{m}$ Be foil was estimated using the calibrated TLD's. The efficiency increases slowly from $\sim 0.2\%$ at 0.2 W/cm^2 to 0.4 at $2 \times 10^{14}\text{ W/cm}^2$. This observed power dependence is very similar to previous measurements made with Nd:glass lasers of comparable irradiance although the absolute conversion efficiency is approximately 20 times greater using the glass laser.⁸ The lower conversion efficiency indicates that the emission originates from a region of lower density than in plasmas created by $1\text{-}\mu\text{m}$ radiation.

The data shown in Fig. 1 were all obtained with less than $100\text{ }\mu\text{J}$ of prepulse energy. Although no systematic dependence of x-ray emission on laser energy for high prepulse energies could be obtained, it was noted that the x-ray emission was significantly decreased if prepulses of energy greater than a few mJ were present.

The spectrum of the continuum was investigated using a number of detector-foil combinations. Figure 2 shows the low-energy portion of a polyethylene $(\text{CH}_2)_n$ spectrum obtained using an array of five surface barrier detectors in conjunction with various foils. The foil thickness and the approximate range of sensitivity for each channel is indicated in Fig. 2. A temperature of $\sim 250\text{ eV}$ may be inferred from the low-energy thermal portion of the spectrum. The higher-energy superthermal portion of the spectrum may be characterized by a temperature of $\sim 9.5\text{ keV}$.

Analysis of line emission was made with flat RAP crystal spectrographs. Typical spectra from Al and Mg targets are shown in Fig. 3.

Figure 3(a) is an 8-shot exposure of emission from a Mg target. Each shot was accompanied by a moderate prepulse of between 10 and 50 mJ in energy. The increase in background at shorter wavelength is caused by fluorescence of the RAP crystal and is an indication that hard x rays are present. The He-like (Mg XI) series and an H-like (Mg XII) line are readily visible in this spectra. Also visible are the accompanying satellite lines, the intercombination lines, and an

Al XII impurity line. Figure 3(b) shows an aluminum spectrum obtained with a 5-shot exposure. In this spectrum, in addition to the He-like resonance lines, the Al K_α fluorescence line is present, an indication that energetic electrons are being emitted from the plasma. Figure 3(c) shows a single-shot-exposure Al spectrum obtained with a small prepulse ($< 10\text{ mJ}$). In this exposure the background and the relative intensity of the K_α line are reduced, the lines are narrower, and a weak H-like resonance line is observable.

If a coronal model is assumed, an estimate of T_e may be obtained from the ratio of He-like to H-like $1s\text{-}2p$ resonance line intensities. For the spectra of Mg and Al a T_e of 400 eV is deduced. Once T_e is known, the electron density (n_e) can be inferred from the ratio of intensities of the $1s\text{-}2p$ He-like resonance and intercombination lines.⁹ For the spectrum shown in Fig. 3(c) this yields an electron density of between 10^{20} and $10^{21}/\text{cm}^3$. At this density it is not unexpected that the coronal model gives a somewhat higher T_e than that derived from the continuum emission spectrum.

Interferometric studies have revealed that when prepulses in excess of 10 mJ are present a plasma of moderate density ($> 10^{18}/\text{cm}^3$) is created in front of the target.⁶ The main pulse is then absorbed further away from the target surface and the density of the x-ray emitting region is lowered. This accounts for the lower x-ray fluxes that are observed in both line emission and continuum spectra when energetic prepulses are present.

The intensity of the observed K_α line does not seem to depend on prepulse energy. This is not unexpected since this line does not originate in the hot-plasma region, but is the result of fluorescence of the cold target material. The energetic electrons responsible for this fluorescence are created at the critical density surface which is situated in front of the primary x-ray emitting region. It is interesting to note that the intensity of the K_α radiation is not very different from that seen in similar experiments with glass lasers, although the relative intensities of the K_α line to resonance line is increased.

We would like to thank D.J. Nagel for his many helpful discussions. We also gratefully acknowledge the able technical support of P. Burtyn and G.A. Berry.

¹E.V. Aglitskii, V.A. Boiko, L.A. Vainshtein, S.M. Zakharov, O.N. Krokhin, and G.V. Sklizkov, *Opt. Spectrosc.* **35**, 558 (1973).

²U. Feldman, G.A. Doschek, D.J. Nagel, R.D. Cowan, and R.R. Whitlock, *Astrophys. J.* **192**, 213 (1974).

³D.T. Attwood, L.N. Coleman, J.T. Larsen, and E.K. Storm, *Phys. Rev. Lett.* **37**, 499 (1976).

⁴B. Yaakobi and A. Nee, *Phys. Rev. Lett.* **36**, 1077 (1976).

⁵M.C. Richardson, N.H. Burnett, H.A. Baldis, G.D. Enright, R. Fedosejevs, N.R. Isenor, and I.V. Tomov, in *Proceedings of the Fourth Workshop on "Laser Interaction and Related Plasma Phenomena"*, Troy, N.Y., 1976 (unpublished).

⁶R. Fedosejevs, I.V. Tomov, N.H. Burnett, G.D. Enright, and M.C. Richardson *Phys. Rev. Lett.* (to be published).

⁷The TLD's were provided and calibrated with the help of G. Charatis of KMS Fusion Inc.

⁸D.J. Nagel, P.G. Burkhalter, C.M. Dozier, B.M. Klein, and R.R. Whitlock, *Bull. Am. Phys. Soc.* **19**, 557 (1974).

⁹V.A. Boiko, S.A. Pikuz, and A.Ya. Faenov, *Sov. J. Quantum Electron.* **5**, 658 (1975).

Far-infrared photoconductivity of uniaxially stressed germanium^{a)}

A. G. Kazanskii^{b)} and P. L. Richards

Department of Physics, University of California, and Materials and Molecular Research Division, Lawrence Berkeley Laboratory, Berkeley, California 94720

E. E. Haller

Department of Instrument Techniques, Lawrence Berkeley Laboratory, Berkeley, California 94720
(Received 20 June 1977; accepted for publication 1 August 1977)

The influence of uniaxial stress on the extrinsic photoconductivity of gallium-doped germanium has been investigated. It has been found that the long-wavelength cutoff is shifted from 114 μm for zero stress to 200 μm for a uniaxial stress of $6.6 \times 10^3 \text{ kg/cm}^2$ along a [100] direction. At this value of stress the responsivity was $\sim 2 \times 10^4 \text{ V/W}$ and the NEP was $\sim 2 \times 10^{-11} \text{ W/Hz}^{1/2}$ at 190 μm .

PACS numbers: 72.40.+w, 81.40.Tv, 85.60.Gz

Germanium doped with various impurities is widely used for sensitive detectors of far-infrared radiation. The choice of the impurity allows one to change the long-wavelength cutoff of such detectors from wavelengths (λ) shorter than 10 μm ¹ for deep impurities to $\lambda = 120 \mu\text{m}$ ² for shallow impurities. For longer wavelengths germanium bolometers are usually used.³ As a rule, however, sensitive germanium bolometers are slower than impurity photoionization detectors, where the rate of response is determined by the recombination processes. It is therefore desirable to extend photoionization detection to longer wavelengths. This can be accomplished by applying uniaxial stress.

This paper describes an investigation of the influence of uniaxial stress on the impurity photoionization of doped germanium. Germanium doped with gallium at a concentration of $2 \times 10^{14} \text{ cm}^{-3}$ and a compensation of less than 0.01 was used in our experiments. Radiation from a Fourier transform spectrometer passed through a stainless-steel light pipe and was concentrated on the sample by a Winston cone.⁴ A cold black polyethylene filter and a Yoshinaga filter were mounted in front of the sample to exclude radiation with wavelengths

shorter than 35 μm and to reduce the influence of background radiation from the top part of the cryostat. The sample and the filters were immersed in liquid helium at 2.0°K. Ohmic contacts were formed by alloying pure In with the germanium at 250°C in an argon atmosphere. The dimensions of the sample were $1 \times 1 \times 6 \text{ mm}$. The stress was applied along the long direction of the sample by a calibrated spring and lever.

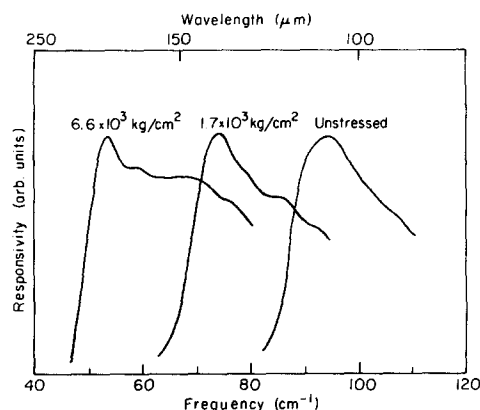


FIG. 1. The spectral responsivity of uniaxially stressed germanium for different values of stress. (The measured spectra were normalized to the output of a Golay detector and then scaled so that the peak responsivity is the same for each.)

^{a)}Work supported by the U.S.E.R.D.A.

^{b)}Permanent address: Department of Physics, Moscow State University, U.S.S.R.